Lane Group–Based Traffic Model for Assessing On-Ramp Traffic Impact

Yen-Yu Chen[1]; Yao Cheng[2]; and Gang-Len Chang, M.ASCE[3]

Abstract: On-ramp merging areas are congestion-prone segments of freeways. Depending on the aggressiveness of the driving population and the congestion level, the speed variance among travel lanes due to lane changes and ramp-merging flows may be so significant as to affect the optimal settings of deployed traffic control systems, such as metering rates or advisory speed limits. Extending from METANET, this study presents a lane group–based (LGB) traffic model to reflect the temporal and spatial distributions of traffic conditions among lane groups. The proposed model would allow traffic engineers to reliably assess the impacts of lane-changing activities in both upstream and downstream segments of an on-ramp area and better design their coordinated control strategies. To assess the effectiveness of the proposed model, this study has compared its performance with METANET under various traffic scenarios. The comparison results show that the proposed model can yield up to 26.9% improvement on the accuracy of predicting the temporal and spatial evolution of a freeway's speed at the interchange area where freeway segments often experience extensive lane-changing activities due to on-ramp merging flows.
DOI: 10.1061/JTEPBS.0000481.

Author keywords: On-ramp area; Lane group–based (LGB) traffic model; Merging impact; Lane-changing impact.

Introduction

Extensive lane-changing maneuvers, triggered by on-ramp merging flows, are well recognized as one main contributor to the formation of a freeway's bottleneck in the interchange area. Over the last several decades, researchers in the traffic community have developed various control strategies to alleviate such bottlenecks. Among those proposed in the literature, a great majority can be classified into the following four major categories: local metering control (Papageorgiou et al. 1991; Zhang and Ritchie 1997; Smaragdis et al. 2004; Gomes and Horowitz 2006; Wang and Papageorgiou 2006), variable speed limit control (Chang et al. 2011; Yang et al. 2015; Seliman et al. 2020), coordinated ramp metering control (Kotsialos et al. 2002; Papamichail et al. 2010a, b; Ghods et al. 2010; Geroliminis et al. 2011; Zhao et al. 2011; Chow and Li 2014; Agarwal et al. 2015), and coordinated control of ramp metering with variable speed limits (Hegyi et al. 2005; Carlson et al. 2010; Frejo and Camacho 2012; Carlson et al. 2014; Li et al. 2017).

Note that the effectiveness of all such control strategies relies on accurate estimations of the freeway's traffic conditions and the resulting capacity reduction in on-ramp areas, which vary with both the on-ramp flow rate and behaviors of the driving population (Yuan et al. 2015). Examples of field studies to confirm such on-ramp merging impacts can be found from the works by Hall and Agyemang-Duah (1991) and Banks (1991). Some later studies have also supported their findings (Cassidy and Bertini 1999; Persaud et al. 1998; Bertini and Malik 2004; Cassidy and Rudjanakanoknad 2005; Chung et al. 2007; Srivastava and Geroliminis 2013).

Hence, in developing effective control strategies, it is critical that the employed traffic model should be capable of realistically capturing both the temporal and spatial impacts by such on-ramp merging flows. In review of most macroscopic traffic models in the literature (e.g., Lighthill and Whitham 1955; Richards 1956; Grewal and Payne 1976; Messner and Papageorgiou 1990; Daganzo 1994; Ngoduy 2006), it is noticeable that METANET model (Messner and Papageorgiou 1990) and cell transmission model (CTM) (Daganzo 1994) are the two mostly used for traffic control applications because of their high computational effectiveness and relatively few parameters. CTM, the first-order approximations of the Lighthill-Whitham-Richards (LWR) model (Lighthill and Whitham 1955; Richards 1956), is reported to be less effective in capturing the capacity drop and the stop-and-go waves at freeway bottlenecks (Spiliopoulou et al. 2014). For the same control needs, Messner and Papageorgiou (1990) developed METANET, a second-order traffic flow model originated from the work by Grewal and Payne (1976). Their model views the target highway under control as a series of interconnected spatial segments (as shown in Fig. 1) and then employs the fundamental relations among flow rate, density, and speed within each segment to project its outgoing flow rate during each time interval. A recent study by Spiliopoulou et al. (2014) concluded that METANET slightly outperformed CTM based on the same data for calibration and validation. Some studies attempted to improve the computational efficiency of METANET for its applications in real-time controls (Groot et al. 2012; Lu et al. 2014; Wang et al. 2020).

However, despite the effectiveness of METANET in projecting the segment-based traffic conditions, it does not distinguish the speed differences among different travel lanes within the same segment. As such, it may yield insufficient information for implementing advanced traffic management strategies, such as lane-based variable speed limit (VSL) control or coordinated ramp metering operations that may require precise lane-by-lane speed

[1]Ph.D. Candidate, Dept. of Civil and Environmental Engineering, Univ. of Maryland, College Park, MD 20742. ORCID: https://orcid.org/0000-0003-0316-0694. Email: yychen804@gmail.com

[2]Faculty Assistant, Dept. of Civil and Environmental Engineering, Univ. of Maryland, College Park, MD 20742 (corresponding author). ORCID: https://orcid.org/0000-0002-0513-0272. Email: chengyao09@gmail.com; ycheng09@umd.edu

[3]Professor, Dept. of Civil and Environmental Engineering, Univ. of Maryland, College Park, MD 20742. Email: gang@umd.edu

Note. This manuscript was submitted on May 17, 2020; approved on September 1, 2020; published online on November 17, 2020. Discussion period open until April 17, 2021; separate discussions must be submitted for individual papers. This paper is part of the ***Journal of Transportation Engineering, Part A: Systems***, © ASCE, ISSN 2473-2907.

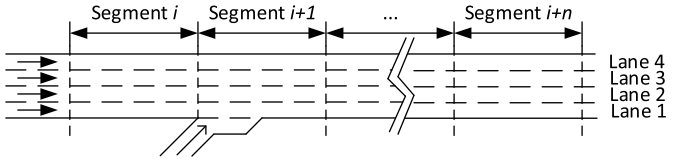

Fig. 1. Macroscopic view of the freeway under the METANET model.

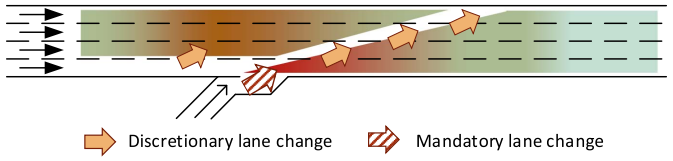

Fig. 2. Graphical illustration of the impacts of the on-ramp merging flows.

and concentration data. Note that the speed variation between travel lanes is especially pronounced on the highway segments upstream and downstream of a ramp, where on-ramp weaving flows may impede the rightmost-lane traffic flows with their mandatory lane changes. Furthermore, these flows will in turn trigger the discretionary lane changes by drivers on the neighboring lanes to avoid the speed reduction and spread the impact. A graphical illustration of such impacts is shown in Fig. 2.

Depending on the aggressiveness of the driving population and the congestion level on the freeway segment, the resulting speed variance among travel lanes due to various lane changes, as shown in Fig. 2, may be so significant as to affect the optimal metering rate or the design of variable speed control strategies. Hence, a freeway traffic model, failing to address such inter-lane discrepancies within the same segment, may not be able to project the spatial and temporal evolution of a ramp's downstream traffic conditions at the desirable level of accuracy for the design of various responsive controls.

To fill such a gap in the existing traffic flow models, this study has proposed a lane group–based (LGB) traffic model, grounded in the core notion of the METANET model. The proposed model is capable of (1) reflecting the speed differences among lane groups within each freeway segment; (2) capturing the impact of the lane-changing behaviors to the speeds of both the target and departing lanes; (3) accounting for the impact of on-ramp merging vehicles on the upstream and downstream segments of the on-ramp; and (4) maintaining high computational efficiency and better accuracy.

METANET Model

As one of the most widely adopted freeway control models, the METANET model (Messner and Papageorgiou 1990) actually views a continuous freeway as a series of conceptually connected segments, in which the vehicles within each segment are assumed to be uniformly distributed. With the assumption and the relation of flow conservation during each time interval, the METANET model can update the temporal and spatial evolution of traffic state for the target freeway with the following core equations:

$$\rho_i(k+1) = \rho_i(k) + \frac{T}{L_i\lambda_i}[q_{i-1}(k) - q_i(k)] \tag{1}$$

$$v_i(k+1) = \min\left\{ v^m, v_i(k) + \frac{T}{\tau}[V_i(\rho_i(k)) - v_i(k)] + \frac{T}{L_i}[v_i(k)v_{i-1}(k) - v_i(k)] - \frac{\upsilon T}{\tau L_i}\frac{[\rho_{i+1},(k) - \rho_i(k)]}{\rho_i(k)+\kappa} \right\} \tag{2}$$

$$V_i(\rho_i(k)) = v_i^f \times \exp\left[-\frac{1}{a_i}\left(\frac{\rho_i(k)}{\rho_i^C}\right)^{a_i}\right] \tag{3}$$

$$q_i(k) = \lambda_i\rho_i(k)v_i(k) \tag{4}$$

where $\rho_i(k)$ and $q_i(k)$ = density and flow rate of Segment i at time k; λ_i and L_i = the number lanes and the length, respectively, on Segment i; v^m = minimum speed; $v_i(k)$ = speed of Segment i at time k; $V_i(\cdot)$, v_i^f, and ρ_i^C denote the function for speed-density relation, the free-flow speed, and critical density, respectively, for Segment i; τ, υ, κ, and a_i = location-specific parameters to be calibrated with field data; and T stands for the time interval for updating the traffic state in each segment.

Note that the convection term in Eq. (2), $T/L_i[v_i(k)v_{i-1}(k) - v_i(k)]$, is to reflect the continuity of traffic conditions between two consecutive freeway segments that are divided for convenience of model computation. Likewise, the anticipation term, $\frac{\upsilon T}{\tau L_i}\frac{[\rho_{i+1},(k)-\rho_i(k)]}{\rho_i(k)+\kappa}$, is proposed to capture the perceivable impacts of the downstream segment's traffic conditions—such as congestion—on the speed of drivers in the current segment.

For those freeway segments with either lane reduction or on-ramps, Messner and Papageorgiou (1990) have suggested to include the following additional terms to reflect their impacts on the traffic flow speeds:

$$-\phi v_i(k)\frac{v_i(k)T\rho_i(k)\Delta\lambda_i}{L_i\lambda_i\rho_i^C} \tag{5}$$

$$-v_i(k)\frac{\delta T r_i(k)}{L_i\lambda_i(k)(\rho_i(k)+\kappa)} \tag{6}$$

where $\Delta\lambda_i$ denotes the number of dropped lanes; $r_i(k)$ indicates the on-ramp flow rate at time k; and ϕ, δ, and κ are parameters to be calibrated with field data.

Conceivably, Eq. (5) is to show that the speed reduction due to lane drops varies with the ratio between the number of vehicles on such lanes [i.e., $v_i(k)T\rho_i(k)\Delta\lambda_i$] and the number of vehicles that Segment i can accommodate under the critical density condition (i.e., $L_i\lambda_i\rho_i^C$). Eq. (6) functions to approximate the speed impact by on-ramp merging flows, based on the ratio between the number of on-ramp vehicles, $Tr_i(k)$, and the number of vehicles in the segment, $L_i\lambda_i(k)\rho_i(k)$.

LGB Traffic Model

Fig. 3 shows the key inputs and principal components of the proposed model grounded in the core logic of the METANET model, including the relations between its key components and primary model outputs. Principal modules of the LGB traffic model, along with their embedded logic relations, are detailed in sequence as follows; all notations for variables used hereafter are provided in Table 1.

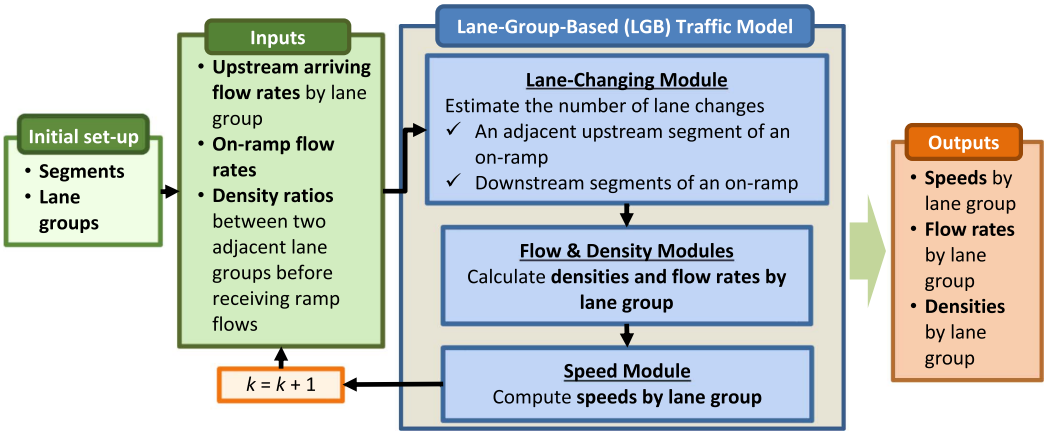

Fig. 3. Key inputs, outputs, and primary components of the LGB traffic model.

Table 1. List of key variables used in the LGB traffic model

Variable	Definition
$\alpha_{j,j+1}$	Target density ratio between Lane groups j and $j+1$
$D_{i,j}$	The set of lane groups in the adjacent *downstream* segment connected to Lane group j in Segment i ($\|D_{i,j}\|$ is the number of lane groups in $D_{i,j}$)
L_i	Length of Segment i
$N_{i,j,j+1}(k)$	Number of vehicles changing from Lane group j to Lane group $j+1$ in Segment i at time k ($j = 1, \ldots, G_i - 1$; G_i is the number of lane groups in Segment i)
$q_{i,j}(k)$	Flow rate of Lane group j in Segment i at time k
$S_{i,j}$	The set of lane groups in the adjacent *upstream* segment connected to Lane group j in Segment i ($\|S_{i,j}\|$ is the number of lane groups in $S_{i,j}$)
T	Time interval for updating the traffic state
$V_i(\cdot)$	Speed-density relation for Segment i
$v_{i,j}(k)$	Speed of Lane group j in Segment i at time k
v^m	Minimum speed
$\lambda_{i,j}$	Number of lanes in Lane group j in Segment i
$\rho_{i,j}(k)$	Density of Lane group j in Segment i at time k (*prior to* receiving lane-changing vehicles)
$\rho^*_{i,j}(k)$	Density of Lane group j of Segment i at time k (after accommodating lane-changing vehicles)
ρ^{jam}	Jam density
ρ^C_i	Critical density of Segment i
$\eta, \tau, \upsilon, \kappa, \phi$	Parameters

Initial System Setup Module

To replicate the complex interactions between freeway ramp and mainline flows from the lane-group view, one needs to first divide the freeway within the control area into several segments (as with the METANET model). Then, travel lanes in a segment are classified into a number of lane groups, based on both the geometric features and speed variance within each segment. Conceivably, one can formulate each lane as one group if the traffic flow speeds vary significantly across lanes.

Note that for convenience of presentation but without loss of the generality, all travel lanes in each freeway segment within the on-ramp control area are classified into three lane groups in the formulation section. As shown in Fig. 4, the rightmost and leftmost lanes are defined as Lane groups 1 and 3, respectively, while all middle lanes are denoted as Lane group 2.

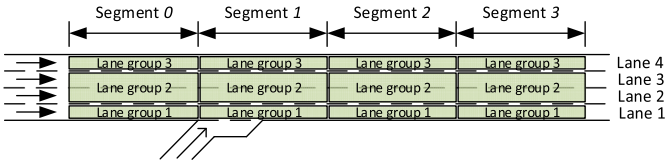

Fig. 4. Freeway segments under the LGB traffic model.

Lane-Changing Module

This module serves to estimate the number of lane changes, based on lane change purposes and the current densities in those lane groups. Eq. (7) shows such dynamics resulted from the number of vehicles performing lane changes in responding to the perceived interference by ramp flows.

$$N_{i,j,j+1}(k) = \begin{cases} \min\left(L_i\rho_{i,j}(k), \eta\lambda_{i+1,j}\lambda_{i+1,j+1}L_{i+1}\dfrac{\rho_{i+1,j}(k) - \rho_{i+1,j+1}(k)}{\lambda_{i+1,j} + \lambda_{i+1,j+1}}, \rho^{jam} - \rho_{i,j+1}(k))L_i\right), & if\ \rho_{i+1,j}(k) > \rho_{i+1,j+1}(k) \\ 0, & otherwise \end{cases} \tag{7}$$

where $N_{i,j,j+1}(k)$ = number of vehicles changing from Lane group j to $j+1$ in Segment i at time k; and η = parameter to reflect the characteristics of driving populations and their reactions to the perceived on-ramp volume.

Note that by setting i and j to 0 and 1, respectively, the second term, $\lambda_{i+1,j}\lambda_{i+1,j+1}L_{i+1}\frac{\rho_{i+1,j}(k)-\rho_{i+1,j+1}(k)}{\lambda_{i+1,j}+\lambda_{i+1,j+1}}$, is to approximate the number of vehicles in Lane group 1 that would perform the lane changes to rebalance the density levels between Lane groups 1 and 2 in view of ramp

flows merging onto the downstream segment's Lane group 1. The third term, $(\rho^{\text{jam}} - \rho_{i,j+1}(k))L_i$, is a straightforward approximation of the available space in Lane group 2 to accommodate such lane-changing vehicles in Segment 0 at time k.

Eq. (8) is to determine the number of lane-changing vehicles in the downstream segments (Segments 1–3) of the on-ramp based on the following assumption: after impacted by the on-ramp merging flows, the vehicles will progressively redistribute its mainline and merged volumes among travel lanes over those downstream segments via drivers' discretionary lane changes until evolving back to the state in which density ratios between neighboring lane groups are approximately the same as those prior to the impacts by on-ramp flows

$$N_{i,j,j+1}(k) = \begin{cases} \min\left(\lambda_{i,j}\lambda_{i,j+1}L_i\dfrac{\rho_{i,j}(k) - \alpha_{j,j+1}\rho_{i,j+1}(k)}{\lambda_{i,j}\alpha_{j,j+1} + \lambda_{i,j+1}}, (\rho^{jam} - \rho_{i,j+1}(k))L_i\right), & if\ \rho_{i,j}(k) > \alpha_{j,j+1}\rho_{i,j+1}(k) \\ 0, & otherwise \end{cases} \tag{8}$$

where $N_{i,j,j+1}(k)$ = number of lane-changing vehicles from Lane group j to $j+1$ in Segment i at time k; and $\alpha_{j,j+1}$ = target density ratio between Lane groups j and $j+1$.

Same as in Eq. (7), the term, $\lambda_{i,j}\lambda_{i,j+1}L_i\frac{\rho_{i,j}(k)-\alpha_{j,j+1}\rho_{i,j+1}(k)}{\lambda_{i,j}\alpha_{j,j+1}+\lambda_{i,j+1}}$, reflects the number of vehicles that need to change lanes from Lane group j to $j+1$ at time k in order to reach the target density ratio between Lane groups j and $j+1$ when $\rho_{i,j}(k)$ is larger than the value of $\alpha_{j,j+1}\rho_{i,j+1}(k)$.

Module for Calculating Flow Rate and Density

Using the flow conservation relation as in METANET, one can formulate the dynamics of density evolution for each lane group as follows:

$$\rho_{i,j}(k+1) = \begin{cases} \rho^*_{i,j}(k) + \dfrac{T}{L_i\lambda_{i,j}}\left[\dfrac{\lambda_{i,j}}{\lambda_{i-1,j}}q_{i-1,j}(k) - q_{i,j}(k)\right], & if \lambda_{i,j} \le \lambda_{i-1,j} \\ \rho^*_{i,j}(k) + \dfrac{T}{L_i\lambda_{i,j}}\left[\left[\sum_{m\in S_{i,j}}\lambda_{i-1,m}q_{i-1,m}(k)\right] - q_{i,j}(k)\right], & if \lambda_{i,j} > \lambda_{i-1,j} \end{cases} \tag{9}$$

$$q_{i,j}(k) = \lambda_{i,j}\rho^*_{i,j}(k)v_{i,j}(k) \tag{10}$$

where $\rho_{i,j}(k+1)$ = density of Lane group j in Segment i at time $k+1$ prior to accommodating the lane-changing vehicles; $\rho^*_{i,j}(k)$ = density of Lane group j of Segment i at time k after receiving those lane-changing vehicles; $\lambda_{i-1,m}$ = number of lanes in Lane group m of the adjacent upstream segment connected to Lane group j of Segment i; and $S_{i,j}$ = set of lane groups in the adjacent upstream segment, which is connected with Lane group j of Segment i.

Note that, the terms $\lambda_{i,j}/\lambda_{i-1,j}q_{i-1,j}(k)$ and $\sum_{m\in S_{i,j}}\lambda_{i-1,m}q_{i-1,m}(k)$ are to reflect the in-flow rate if the number of lanes for each lane group differs between successive segments. Also, note that $\rho^*_{i,j}(k)$ in Eqs. (9) and (10) denotes the density after receiving the lane-changing vehicles, as shown in Eq. (11)

$$\rho^*_{i,j}(k) = \rho_{i,j}(k) + \frac{N_{i,j-1,j}(k) - N_{i,j,j+1}(k)}{L_i\lambda_{i,j}} \tag{11}$$

where $N_{i,j-1,j}(k) - N_{i,j,j+1}(k)$ = net number of vehicles changing into Lane group j in Segment i at time k. For the rightmost lane group, $N_{i,j-1,j}(k)$ equals 0. In addition, for the leftmost lane group, $N_{i,j,j+1}(k)$ is equal to 0.

Speed Update Module

Again, by replacing the segment-based notion in METANET with specific lane-group relations, one can reformulate the speed dynamics for each lane group as follows:

$$\begin{aligned} v_{i,j}(k+1) = \min\Bigg\{ & v^m, v_{i,j}(k) + \frac{T}{\tau}[V_i(\rho^*_{i,j}(k)) - v_{i,j}(k)] \\ & + \frac{T}{L_i}v_{i,j}(k)\left[\frac{\sum_{m\in S_{i,j}}(v_{i-1,m}(k))}{|S_{i,j}|} - v_{i,j}(k)\right] \\ & - \frac{\upsilon T}{\tau L_i}\frac{\left[\frac{\sum_{w\in D_{i,j}}(\rho^*_{i+1,w}(k))}{|D_{i,j}|} - \rho^*_{i,j}(k)\right]}{\rho^*_{i,j}(k) + \kappa} \\ & - \frac{\phi\max(v_{i,j}(k) - v_{i,j-1}(k), 0)N_{i,j-1,j}(k)}{L_i\lambda_{i,j}\rho^C_i}\Bigg\} \end{aligned} \tag{12}$$

where $v_{i,j}(k)$ = speed of Lane group j in Segment i at time k; $D_{i,j}$ = set of lane groups in the adjacent downstream segment, which are connected with Lane group j of Segment i ($|D_{i,j}|$ is the number of lane groups in $D_{i,j}$); $N_{i,j-1,j}(k)$ = number of lane-changing vehicles from Lane group $j-1$ to Lane group j in Segment i at time k; ρ^C_i = critical density of Segment i; and τ, υ, κ, and ϕ = parameters to be calibrated.

Note that the last term, $-\phi\max(v_{i,j}(k) - v_{i,j-1}(k), 0)N_{i,j-1,j}(k)/L_i\lambda_{i,j}\rho^C_i$, in Eq. (12) is proposed to reflect the impacts of lane changes in each lane group on its resulting speed that increases with the speed difference between lane groups and the frequency of such changes. The functional form of the speed-density relationship of Segment i is the same as Eq. (3).

To reflect the on-ramp merging impacts on the directly connected lane group's speed, one can add an extra term, $-v_{i,1}(k)\frac{\delta Tr_i(k)}{L_i(\rho^*_{i,1}(k)+\kappa)}$, to Eq. (12), indicating that such impacts increase with the ratio between the number of on-ramp vehicles, $Tr_i(k)$, and the number of vehicles in the lane group, $L_i\rho^*_{i,1}(k)$.

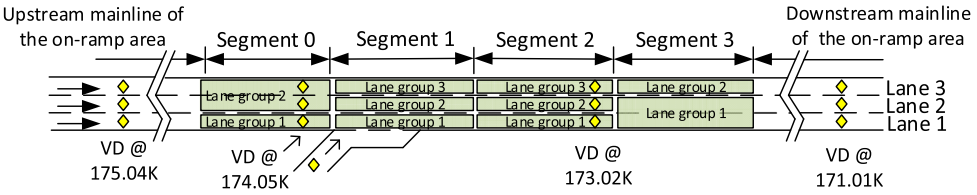

Fig. 5. Locations of the detectors and segmentation.

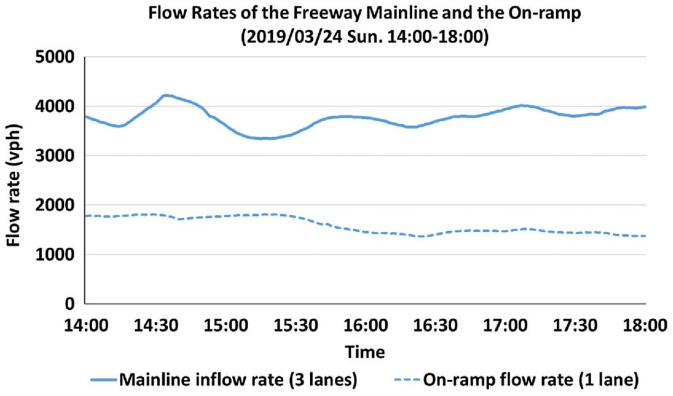

Fig. 6. Flow rates of the freeway mainline measured at 175.04 K and the on-ramp. vph = vehicles per hour.

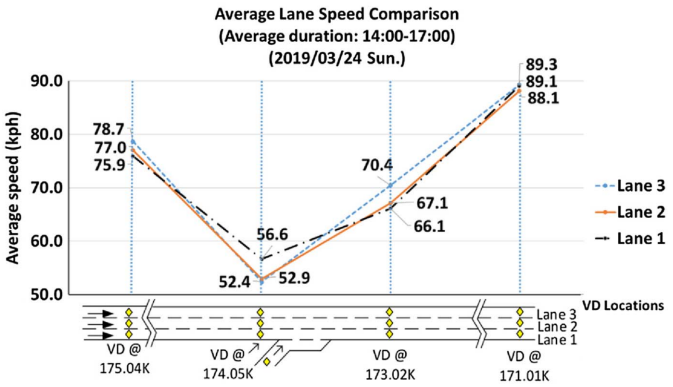

Fig. 7. Average lane speed comparison before and after the on-ramp.

Note that such impacts due to on-ramp merging under the METANET model are assumed to evenly distribute over all lanes in the segment. In contrast, the proposed model first captures such impacts with the directly connected lane group. The impacts are then propagated through the estimation of lane-group density before and after receiving the lane-changing vehicles between lane groups in the same segment and the downstream segments.

Model Evaluation with Field Data

Fig. 5 shows the geometric features and vehicle detector (VD) locations of a freeway on-ramp area from Taiwan Freeway No-1 for calibration and evaluation of the proposed LGB traffic model. The entire area for field study has been divided into four segments, about 500 m each in length, based on the ramp location and exhibited lane-changing activities. Those three travel lanes in each segment are further grouped into two or three lane groups, as shown in Fig. 5, using the information of detected speed and flow rate distribution across all lanes.

Fig. 6 illustrates the temporal distribution of ramp and mainline flow rates on a typical day, and Fig. 7 highlights the significant speed reduction on Segments 0 and 2 due to the on-ramp waving flows and vehicles performing discretionary lane changes.

Some key data associated with the target freeway segment for evaluation are summarized as follows:

- Date of data for calibration: 2–6 p.m. on March 17, 2019
- Date of data for evaluation: 2–6 p.m. on March 24, 2019
- Collected traffic flow data: speed (km/h) and flow rate [vehicles per hour (vph)] per lane per minute from detectors at 174.05 km and 173.02 km
- Average freeway mainline flow rate: 3,400–4,200 vph for all lanes
- Average ramp flow rate: 1,400–1,800 vph (Fig. 6)
- Speed limit: 110 km/h

Evaluation Results at the Lane-Group Level

To evaluate the proposed model's unique feature, the performance evaluation first compares the predicted traffic conditions by lane group with those measured by the two sets of detectors, based on the following three statistics: mean absolute error (MAE), mean absolute percentage error (MAPE), and Theil's inequality coefficient (Koutsoyiannis 1973), as shown in Eq. (13). Note that Theil's inequality coefficient is adopted in this study because it can concurrently measure the discrepancy between the prediction values and field data caused by the difference between their means and variances. The benefits of deriving the segment-based average traffic conditions from the LGB results will also be demonstrated by the performance comparisons between the proposed model and METANET

$$Theil's\ Inequality\ Coefficient{:}U = \sqrt{\frac{\sum (P_i - A_i)^2/n}{\sum A_i^2/n}} 0 \le U \le \infty \tag{13}$$

where P_i = predicted values; A_i = actual values; n = number of data points; and the model is viewed to attain perfect forecasts if $U = 0$ (i.e., $P_i = A_i$).

As given in Table 2, the obtained Theil's inequality coefficients with respect to speeds and flow rates at both detector locations over all lane groups are all far less than 1, reflecting that the predicted traffic states, before and after impacted by the on-ramp flows, are sufficiently close to the detected field data. Such desirable properties for traffic state prediction can also be seen from the resulting MAEs, which are less than 4 km/h for the speeds and below three

Table 2. Comparison results with respect to LGB speeds and flow rates

Indicator	At 174.05 K		At 173.02 K		
	Lane group 1	Lane group 2	Lane group 1	Lane group 2	Lane group 3
Theil's inequality coefficient					
Speed	0.0721	0.0835	0.0569	0.0555	0.0600
Flow rate	0.1014	0.0620	0.0469	0.0531	0.0605
Mean absolute error (MAE)					
Speed (km/h)	3.87	3.88	3.43	3.28	3.82
Flow rate (vehicle/min)	1.27	2.20	0.93	1.32	1.55
Mean absolute percentage error (MAPE)					
Speed (%)	6.3	6.7	4.8	4.6	5.1
Flow rate (%)	7.2	4.8	3.6	4.1	5.0

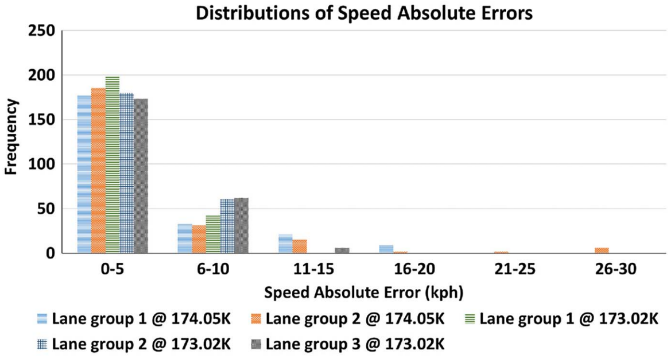

Fig. 8. Distributions of the estimated absolute errors for speed by lane group.

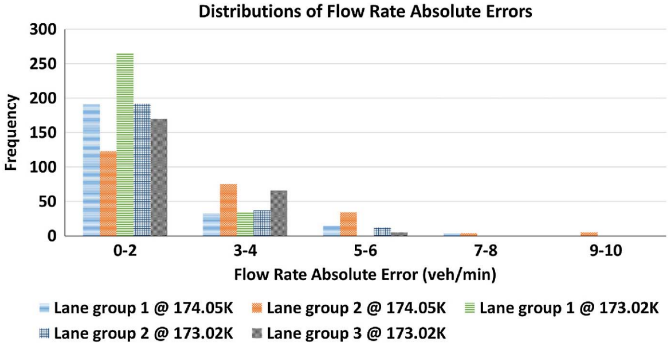

Fig. 9. Distributions of estimated absolute errors for flow rate by lane group.

vehicles per minute for the predicted flow rates on all lane groups at the location of 174.05 K and 173.02 K. Most of such predicted deviations across all lane groups at both detector locations are less than 5 km/h for the predicted speed deviation (Fig. 8), and 94% of the differences with the detected flow rate are within the range of four vehicles per minute (Fig. 9).

Note that approximately the same level of very low MAEs for the freeway's traffic states, before and after merging of ramp flows, confirms the proposed model's effectiveness in capturing the impacts of mainline vehicles' lane-changing maneuvers and ramp flows' merging frequency on the resulting speed and flow rate at the lane-group level.

As for the model performance with MAPE, the predicted errors for lane-group speed with the proposed model range from the lowest of 4.6% for Lane group 2 at the location of 173.02 K to the highest of 6.7% for Lane group 2 at the location of 174.05 K. The MAPEs for flow rate prediction for all lane groups at both locations are all within the range of 5%, except for the 7.2% for Lane group 1 at 174.05 K where there are heavy discretionary lane-changing activities.

In brief, considering the data accuracy from most existing traffic detectors, one can expect that the proposed model offers sufficient accuracy for the traffic engineers to take full advantage of available sensor information and to best design the freeway control strategies at the lane-group level.

Evaluation Results at the Segment Level

To assess the benefits of applying the proposed LGB traffic model for predicting the average flow rate and speed across all lanes as in most existing models, the study has further compared its performance at the segment level with respect to speed and flow rates using the field data averaged from all lane detectors. The results from the well-established METANET model have also been computed to serve as the baseline for assessing the proposed model's performance improvement. The parameter settings adopted in the LGB model and METANET are provided in Tables 3–6, respectively.

As given in Table 7, the predicted average flow rates over all lanes by both the proposed model and METANET at two detector stations are at the same high level of accuracy, based on the statistics of Theil's inequality coefficient (i.e., less than 0.1). However, the prediction accuracy of the proposed LGB traffic model with respect to the average speeds at the segment level clearly outperforms METANET, and is comparable to its prediction accuracy for the average flow rate (also less than 0.1). Such interesting findings confirm the observations that the lane-changing maneuvers in a freeway's interchange area due to the on-ramp merging flows indeed often exhibit substantial speed variance between travel lanes. Consequently, such observations justify the need to employ the LGB traffic model for estimating the projected speeds for either individual lane groups or across all lanes.

In contrast, as for use in projecting the average flow rate over all lanes, the segment-based model, such as METANET, appears to achieve the same quality of prediction as with the proposed LGB traffic model that produces the average from all lane groups. Note that the performance discrepancy between these two models with respect to the speed and flow rate is consistent with the field observation that the impedance-creating lane-changing vehicles will inevitably cause speed variation between travel lanes.

Table 3. Parameter settings of LGB model for all lane groups

Parameter	Value
τ (s)	23
δ	0.012
υ (km^2/h)	50
ϕ	2.6
κ (vehicle/km)	40

Table 4. Lane group–based parameter settings of LGB model

Segment	Lane group	$v_{i,j}^f$ (km/h)	$\rho_{i,j}^C$ (vehicle/km/lane)	$a_{i,j}$	η	$\alpha_{j,j+1}$
0	1	109	29	2	1	—
	2	113	29	2	—	—
1	1	100	25	2	—	1
	2	100	25	2	—	1
	3	115	29	2.2	—	—
2	1	100	27	2.2	—	1
	2	100	27	2.3	—	1
	3	110	30	2.7	—	—
3	1	105	31	2.2	—	1
	2	105	31	2.2	—	—

Table 5. Parameter settings of METANET for all segments

Parameter	Value
τ (s)	23
δ	0.012
υ (km^2/h)	50
κ (vehicle/km)	35

Table 6. Segment-based parameter settings of METANET

Segment	v_i^f (km/h)	ρ_i^C (vehicle/km/lane)	a_i
0	111	29	2
1	105	26	2.1
2	103	28	2.4
3	105	31	2.2

Table 7. Validation results of speed and flow rate between the proposed model and METANET

Indicator	Proposed model	METANET model	Percentage improvement (%)
Theil's inequality coefficient			
Speed			
At 174.05 K	0.0946	0.3478	72.8[a]
At 173.02 K	0.0484	0.1463	66.9[a]
Flow rate			
At 174.05 K	0.0570	0.0572	0.3[a]
At 173.02 K	0.0392	0.0452	13.3[a]
Mean absolute error (MAE)			
Speed (km/h)			
At 174.05 K	3.97	16.17	75.4[a]
At 173.02 K	2.88	7.80	63.1[a]
Flow rate (vehicle/min)			
At 174.05 K	3.10	3.04	−2.0[a]
At 173.02 K	2.94	3.46	15.0[a]
Mean absolute percentage error (MAPE)			
Speed (%)			
At 174.05 K	7.0%	33.9%	26.9[b]
At 173.02 K	4.1%	11.5%	7.4[b]
Flow rate (%)			
At 174.05 K	4.9%	4.8%	−0.1[b]
At 173.02 K	3.3%	3.9%	0.6[b]

[a](The indicator value of METANET—The indicator value of the proposed model)/the indicator value of METANET × 100 (%).
[b]The MAPE of METANET—The MAPE of the proposed model.

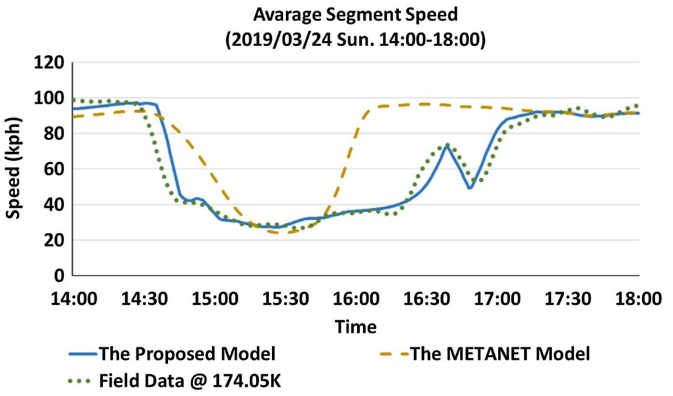

Fig. 10. Speed comparison among the proposed model, METANET model, and field data (at 174.05 K).

In consequence, the resulting average speed may differ significantly from that with the segment-based method grounded on the uniformity assumption of traffic conditions across all lanes. However, since all such lane changes, triggered by on-ramp flows, occur mainly between lanes (less likely to be in subsequent segments), it is expected that the number of vehicles within the same freeway segment ought to remain at approximately the same level. Hence, the total flow rate for all lanes, insensitive to the lane-changing frequency within the same segment, can be predicted to the acceptable level of accuracy with either the segment-based model or the LGB model.

Note that the aforementioned findings with respect to the performance of the proposed model and METANET are further supported by the evaluation results with MAE and MAPE, as given in Table 7. For instance, at the location of 174.05 K, both models yield the same level of accuracy in MAE (i.e., about 2% in difference) for the flow rate prediction, but vary significantly in their forecasts of the average speed (i.e., MAE of 3.97 km/h versus 16.17 km/h). The same conclusions can also be made from the comparison results with MAPE.

The performance discrepancy between these two models can be further verified with the comparison to the detector data shown in Figs. 10 and 11. Noticeably, the proposed model (but not the METANET model) can replicate the drop in average speed from 14:30 to 15:30 at the location of 174.05 K, where many drivers may have exercised lane changes to avoid the speed impedance by on-ramp flows. Such a speed-drop pattern, triggered by lane-changing activities, is often followed by a slow recovery process, as shown in its temporal evolution during the time period between 15:30 and 17:30, due likely to propagation of the impacts by the

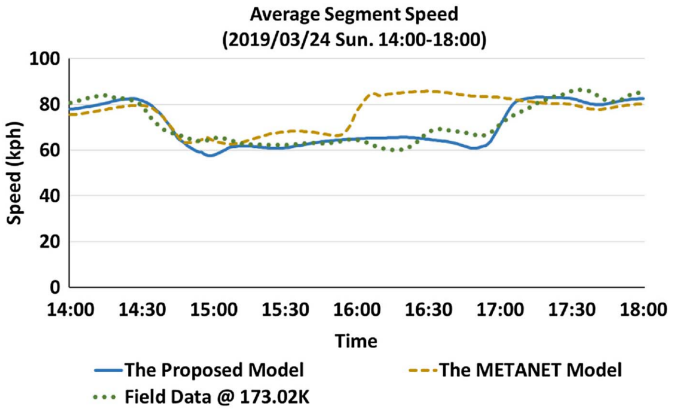

Fig. 11. Speed comparison among the proposed model, METANET model, and field data (at 173.02 K).

on-ramp merging flows measured at the downstream location of 173.02 K.

Fig. 11 further illustrates the temporal evolution patterns of the average flow speed at the freeway segment of 173.02 K, produced from both models and the detectors, where most on-ramp flows may have merged onto the mainline segment. Again, it is evident that the proposed LGB traffic model can better capture the impacts incurred by the ramp flows and those mainline vehicles exercising discretionary lane changes on both the freeway segment's average speed and the speed variance across lanes. Finally, it is worth noting that the overall traffic impacts by the on-ramp flows on the upstream segment (e.g., at 174.05 K) seem more pronounced than on the ramp's downstream segment (e.g., at 173.02 K). Such observation reflects the need to employ some information strategies to advise drivers to take early-lane changes so as to minimize the resulting impacts on the overall traffic conditions.

Sensitivity Analysis

Compared to the METANET model, the proposed model has introduced two critical parameters to describe the lane change behaviors:

- η: the lane change parameter for the upstream segment of an on-ramp (i.e., Segment 0)
- $\alpha_{j,j+1}$: the lane change parameter for the downstream segments (i.e., Segments 1–3)

These two parameters may affect the number of lane changes and consequently impact the resulting lane speeds and their distributions. To test the performance of the proposed model under different sets of such parameters, this study has further conducted an extensive sensitivity analysis.

In conducting such sensitivity analyses, the focus is to investigate the variation of the average speed under the following scenarios: that is, $\pm 20\%$, $\pm 40\%$, and $\pm 60\%$ to each key parameter.

The results are shown in Figs. 12 and 13, and the main findings are summarized as follows:

1. When the parameter η (i.e., lane change parameter of Segment 0) fluctuates by 20%, the average speeds of all lane groups remain quite stable (Fig. 12).
2. As shown in Fig. 12, a decrease in η (i.e., decreasing the willingness of lane changes from Lane group 1 to Lane group 2 in Segment 0) will result in a reduction of the average speed of lane groups in Segment 0. The reason is that increasing the number of vehicles staying in Lane group 1 would reduce the speed of the lane group and further affect the speed of adjacent Lane group 2. Furthermore, due to the interdependent relation between consecutive lane groups, the average speeds of lane groups in the further downstream segments (Segments 1–3) will also decrease under such a scenario. In addition, the speed reduction percentages diminish with the distance. For example, the speed of Lane group 1 of Segment 1 decreases by 12.2% when η decreases by 60%. By contrast, the counterpart of Segment 3 (a further downstream segment) remains quite stable.
3. As shown in Fig. 12, when increasing η (i.e., increasing the willingness of lane changes from Lane group 1 to Lane group 2 in Segment 0), the average speed of lane groups in Segment 0 also decreases. The reason is that the increasing number of vehicles changing to Lane group 2 results in a slower speed of the receiving lane group, and further impacts the speed of Lane group 1. Therefore, the percentage reduction in the speed of Lane group 2 is slightly higher than the counterpart of Lane group 1. For example, the speed of Lane group 1 in Segment 0 decreases by 3.6%, while the counterpart of Lane group 2 drops by 4.7% under the scenario of a 60% increase of η.
4. Decreasing the lane-changing parameter of Segments 1–3 (i.e., $\alpha_{j,j+1}$) indicates an increase in the willingness of lane

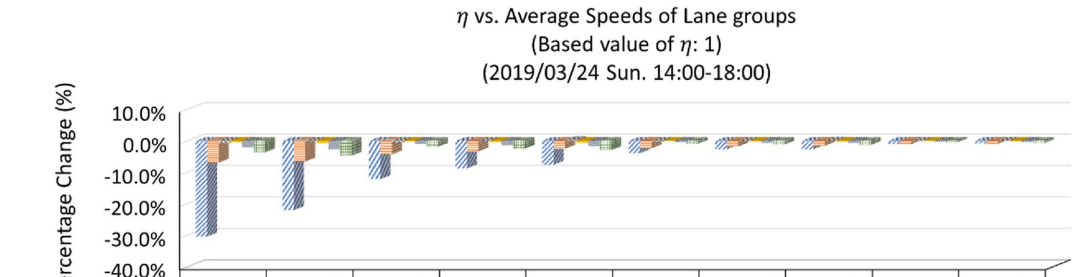

	LG 1 of segment 0	LG 2 of segment 0	LG 1 of segment 1	LG 2 of segment 1	LG 3 of segment 1	LG 1 of segment 2	LG 2 of segment 2	LG 3 of segment 2	LG 1 of segment 3	LG 2 of segment 3
Based value - 60%	-30.4%	-22.1%	-12.2%	-8.8%	-7.6%	-3.9%	-2.7%	-2.7%	-1.0%	-0.8%
Based value - 40%	-6.9%	-6.5%	-4.3%	-3.4%	-2.5%	-2.3%	-1.8%	-1.5%	-1.0%	-0.9%
Based value - 20%	-0.6%	-0.1%	-0.4%	0.0%	0.2%	-0.2%	0.0%	0.0%	-0.1%	0.0%
Based value + 20%	-0.4%	-0.7%	-0.1%	-0.4%	-0.6%	0.0%	-0.2%	-0.2%	0.0%	-0.1%
Based value + 40%	-1.9%	-2.7%	-0.9%	-1.4%	-1.7%	-0.4%	-0.6%	-0.7%	-0.2%	-0.4%
Based value + 60%	-3.6%	-4.7%	-1.9%	-2.5%	-2.9%	-0.9%	-1.2%	-1.3%	-0.5%	-0.7%

Lane group of the segment

Fig. 12. Relative changes in average speed over η (lane change parameter of Segment 0). LG = lane group.

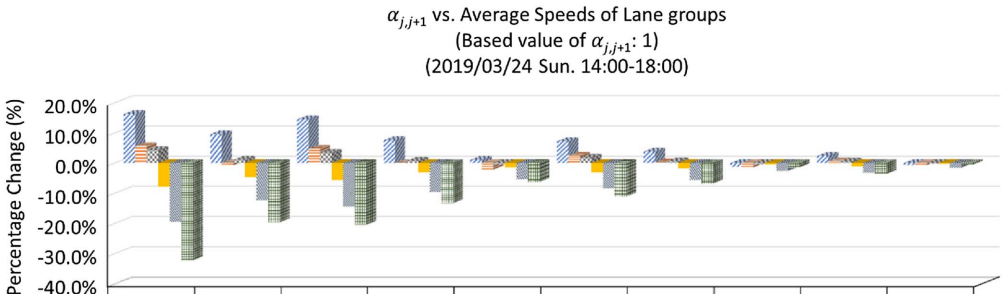

	LG 1 of segment 0	LG 2 of segment 0	LG 1 of segment 1	LG 2 of segment 1	LG 3 of segment 1	LG 1 of segment 2	LG 2 of segment 2	LG 3 of segment 2	LG 1 of segment 3	LG 2 of segment 3
Based value - 60%	16.2%	9.6%	14.5%	7.6%	1.1%	7.2%	3.8%	-1.3%	2.3%	-0.7%
Based value - 40%	5.6%	-0.9%	4.7%	-0.1%	-2.2%	2.4%	0.2%	-1.5%	0.5%	-0.8%
Based value - 20%	4.3%	1.1%	3.3%	0.8%	-0.4%	1.7%	0.5%	-0.5%	0.5%	-0.2%
Based value + 20%	-7.9%	-4.7%	-5.7%	-3.1%	-1.4%	-3.1%	-1.8%	-0.4%	-1.1%	-0.3%
Based value + 40%	-19.4%	-12.3%	-14.4%	-9.6%	-5.4%	-8.4%	-5.6%	-2.6%	-3.2%	-1.5%
Based value + 60%	-32.2%	-19.6%	-20.5%	-13.3%	-6.3%	-11.1%	-6.8%	-1.4%	-3.6%	-0.5%

Lane group of the segment

Fig. 13. Relative changes in average speed over $\alpha_{j,j+1}$ (lane change parameter of Segments 1–3).

changes from Lane group j to Lane group $j+1$. As such, the on-ramp vehicles would be likely to distribute to inner lane groups faster, and thus improve the speed of the outermost lane group (i.e., Lane group 1). Such lane-changing patterns will further propagate the speed impacts to the inner lane groups in the same segment. For example, the speeds of Lane groups 1, 2, and 3 on Segment 1 increase by 14.5%, 7.6%, and 1.1%, respectively, when $\alpha_{j,j+1}$ decreases by 60%, as shown in Fig. 13.

5. By contrast, the willingness of lane changes from Lane group j to Lane group $j+1$ in downstream segments (i.e., Segments 1–3) shows a decrease with an increase in $\alpha_{j,j+1}$ (Fig. 13). As such, more vehicles will stay in Lane group 1, and thus decrease the speeds of this lane group and further trigger such impacts on the speeds of the other lane groups. For instance, the values of the parameter increasing by 40% and 60% will provoke the speeds of Lane group 1 of Segment 1 to decrease by 14.4% and 20.5%, respectively. Also, as shown in Fig. 13, such parameter changes will further cause the speed reduction in the other lane groups sharing the same segment.
6. Because Segment 1 is the one connected to the on-ramp, it will expectedly receive the most significant impact among all downstream segments (i.e., Segments 1–3) when experiencing the changes of $\alpha_{j,j+1}$ (Fig. 13).
7. As expected, the speeds of lane groups in Segment 0 are positively correlated with the speeds of its adjacent downstream lane groups (i.e., lane groups of Segment 1). For example, as shown in Fig. 13, a reduction of 60% in $\alpha_{j,j+1}$ will concurrently increase the speed of Lane group 1 in Segment 0 by 16.2% and its downstream lane group (i.e., Lane group 1 of Segment 1) by 14.5%.

Conclusions

We fully recognized that METANET has been developed to account for the balance between model complexity and potential contributions of the output information in developing control strategies. Grounded on its accomplishment, this study intends to highlight the potential of extending its segment-based logic to LGB formulations when data are available. Such an extension can better capture the complex on-ramp weaving impacts to the extent possible and offer more information for the development of congestion-mitigating strategies for the interchange areas. The results of the lane group–level evaluation indicate that the proposed LGB model can offer sufficient accuracy for traffic engineers to take full advantage of available sensor information in estimating the temporal and spatial evolution of speeds across all lane groups within the interchange area.

The produced lane-specific traffic information is especially valuable for design of control strategies for highway segments experiencing extensive lane-changing maneuvers due to either on-ramp merging flows or off-ramp queue spillback. Some examples of its potential applications include:

1. Local or coordinated ramp metering control: The information of both speed and density variations across all travel lanes is essential for computing the remaining capacities of the freeway's rightmost lanes in merging areas, and for setting the proper metering rates.
2. Lane-based variable speed control: One can apply the estimated lane-group speed data to integrate ramp metering with the lane-based variable speed control to contend with recurrent congestion plaguing most commuting freeway corridors.
3. Off-ramp signal design: The speed data on each lane is essential for estimation of vehicle delays caused by off-ramp queue spillback, which should be taken into account in the optimal design of off-ramp signals during peak periods.
4. Estimating the impacts of work-zone configuration on traffic safety and delays: The proposed lane-group system can serve as a tool for estimating the impacts of work-zone configuration on the resulting traffic conditions, including the queue length, speed, concentration, and potential collisions in the open and closed lanes. With the estimated lane-specific traffic conditions, traffic engineers can better assess what control strategies to take (e.g., early, late, and dynamic merge), and when and where to activate the control.
5. Incident management: During nonrecurrent congestion caused by incidents, traffic conditions estimated with the LGB system can better predict its impact range and duration, allowing the engineers to better design the control strategies.

To facilitate applications of the proposed LGB traffic model, our ongoing research in this regard will include:

1. The development of an automated model calibration system with field data.
2. More field tests with lane-based data to demonstrate its effectiveness in practice and identify any issue for further enhancement.
3. Integration with ramp metering to constitute a local freeway control system operated at either the time-of-day or real-time mode.
4. The extension of the LGB concept to off-ramp segments enables it to serve as a useful traffic state prediction model that can be adopted in a large-scale coordinated freeway control system.

Data Availability Statement

Some or all data, models, or code that support the findings of this study, such as speed and flow rates, are available from the corresponding author upon reasonable request.

References

Agarwal, S., P. Kachroo, S. Contreras, and S. Sastry. 2015. "Feedback-coordinated ramp control of consecutive on-ramps using distributed modeling and Godunov-based satisfiable allocation." *IEEE Trans. Intell. Transp. Syst.* 16 (5): 2384–2392. https://doi.org/10.1109/TITS.2015.2398453.

Banks, J. H. 1991. "Two-capacity phenomenon at freeway bottlenecks: A basis for ramp metering?" *Transp. Res. Rec.* 1320: 83–90.

Bertini, R. L., and S. Malik. 2004. "Observed dynamic traffic features on freeway section with merges and diverges." *Transp. Res. Rec.* 1867 (1): 25–35. https://doi.org/10.3141/1867-04.

Carlson, R. C., I. Papamichail, and M. Papageorgiou. 2014. "Integrated feedback ramp metering and mainstream traffic flow control on motorways using variable speed limits." *Transp. Res. Part C: Emerging Technol.* 46 (Sep): 209–221. https://doi.org/10.1016/j.trc.2014.05.017.

Carlson, R. C., I. Papamichail, M. Papageorgiou, and A. Messmer. 2010. "Optimal motorway traffic flow control involving variable speed limits and ramp metering." *Transp. Sci.* 44 (2): 238–253. https://doi.org/10.1287/trsc.1090.0314.

Cassidy, M. J., and R. L. Bertini. 1999. "Some traffic features at freeway bottlenecks." *Transp. Res. Part B: Methodol.* 33 (1): 25–42. https://doi.org/10.1016/S0191-2615(98)00023-X.

Cassidy, M. J., and J. Rudjanakanoknad. 2005. "Increasing the capacity of an isolated merge by metering its on-ramp." *Transp. Res. Part B: Methodol.* 39 (10): 896–913. https://doi.org/10.1016/j.trb.2004.12.001.

Chang, G. L., S. Y. Park, and J. Paracha. 2011. "Intelligent Transportation system field demonstration: Integration of variable speed limit control and travel time estimation for a recurrently congested highway." *Transp. Res. Rec.* 2243 (1): 55–66. https://doi.org/10.3141/2243-07.

Chow, A. H., and Y. Li. 2014. "Robust optimization of dynamic motorway traffic via ramp metering." *IEEE Trans. Intell. Transp. Syst.* 15 (3): 1374–1380. https://doi.org/10.1109/TITS.2014.2310454.

Chung, K., J. Rudjanakanoknad, and M. J. Cassidy. 2007. "Relation between traffic density and capacity drop at three freeway bottlenecks." *Transp. Res. Part B: Methodol.* 41 (1): 82–95. https://doi.org/10.1016/j.trb.2006.02.011.

Daganzo, C. F. 1994. "The cell transmission model: A dynamic representation of highway traffic consistent with the hydrodynamic theory." *Transp. Res. Part B: Methodol.* 28 (4): 269–287. https://doi.org/10.1016/0191-2615(94)90002-7.

Frejo, J. R. D., and E. F. Camacho. 2012. "Global versus local MPC algorithms in freeway traffic control with ramp metering and variable speed limits." *IEEE Trans. Intell. Transp. Syst.* 13 (4): 1556–1565. https://doi.org/10.1109/TITS.2012.2195493.

Geroliminis, N., A. Srivastava, and P. Michalopoulos. 2011. "A dynamic-zone-based coordinated ramp-metering algorithm with queue constraints for Minnesota's freeways." *IEEE Trans. Intell. Transp. Syst.* 12 (4): 1576–1586. https://doi.org/10.1109/TITS.2011.2164792.

Ghods, A. H., L. Fu, and A. Rahimi-Kian. 2010. "An efficient optimization approach to real-time coordinated and integrated freeway traffic control." *IEEE Trans. Intell. Transp. Syst.* 11 (4): 873–884. https://doi.org/10.1109/TITS.2010.2055857.

Gomes, G., and R. Horowitz. 2006. "Optimal freeway ramp metering using the asymmetric cell transmission model." *Transp. Res. Part C: Emerging Technol.* 14 (4): 244–262. https://doi.org/10.1016/j.trc.2006.08.001.

Grewal, M. S., and H. J. Payne. 1976. "Identification of parameters in a freeway traffic model." *IEEE Trans. Syst. Man Cybern.* 3: 176–185. https://doi.org/10.1109/TSMC.1976.5409233.

Groot, N., B. De Schutter, and H. Hellendoorn. 2012. "Integrated model predictive traffic and emission control using a piecewise-affine approach." *IEEE Trans. Intell. Transp. Syst.* 14 (2): 587–598. https://doi.org/10.1109/TITS.2012.2227314.

Hall, F. L., and K. Agyemang-Duah. 1991. "Freeway capacity drop and the definition of capacity." *Transp. Res. Rec.* 1320: 91–98.

Hegyi, A., B. De Schutter, and H. Hellendoorn. 2005. "Model predictive control for optimal coordination of ramp metering and variable speed limits." *Transp. Res. Part C: Emerging. Technol.* 13 (3): 185–209. https://doi.org/10.1016/j.trc.2004.08.001.

Kotsialos, A., M. Papageorgiou, M. Mangeas, and H. Haj-Salem. 2002. "Coordinated and integrated control of motorway networks via nonlinear optimal control." *Transp. Res. Part C: Emerging. Technol.* 10 (1): 65–84. https://doi.org/10.1016/S0968-090X(01)00005-5.

Koutsoyiannis, A. 1973. *Theory of econometrics: An introductory exposition of econometric methods*. London: McMillan.

Li, Z., P. Liu, C. Xu, H. Duan, and W. Wang. 2017. "Reinforcement learning-based variable speed limit control strategy to reduce traffic congestion at freeway recurrent bottlenecks." *IEEE Trans. Intell. Transp. Syst.* 18 (11): 3204–3217. https://doi.org/10.1109/TITS.2017.2687620.

Lighthill, M. J., and G. B. Whitham. 1955. "On kinematic waves II. A theory of traffic flow on long crowded roads." *Proc. R. Soc. London, Ser. A* 229 (1178): 317–345. https://doi.org/10.1098/rspa.1955.0089.

Lu, X. Y., T. Z. Qiu, R. Horowitz, A. Chow, and S. Shladover. 2014. "METANET model improvement for traffic control." *Int. J. Transp.* 2 (2): 65–88. https://doi.org/10.14257/ijt.2014.2.2.05.

Messner, A., and M. Papageorgiou. 1990. "METANET: A macroscopic simulation program for motorway networks." *Traffic Eng. Control* 31 (9): 466–470.

Ngoduy, D. 2006. "Macroscopic discontinuity modeling for multiclass multilane traffic flow operations." M.Sc. thesis, Dept. of Civil Engineering, Delft Univ. of Technology.

Papageorgiou, M., H. Hadj-Salem, and J. M. Blosseville. 1991. "ALINEA: A local feedback control law for on-ramp metering." *Transp. Res. Rec.* 1320 (1): 58–67.

Papamichail, I., A. Kotsialos, I. Margonis, and M. Papageorgiou. 2010a. "Coordinated ramp metering for freeway networks—A model-predictive hierarchical control approach." *Transp. Res. Part C: Emerging Technol.* 18 (3): 311–331. https://doi.org/10.1016/j.trc.2008.11.002.

Papamichail, I., M. Papageorgiou, V. Vong, and J. Gaffney. 2010b. "Heuristic ramp-metering coordination strategy implemented at Monash freeway, Australia." *Transp. Res. Rec.* 2178 (1): 10–20. https://doi.org/10.3141/2178-02.

Persaud, B., S. Yagar, and R. Brownlee. 1998. "Exploration of the breakdown phenomenon in freeway traffic." *Transp. Res. Rec.* 1634 (1): 64–69. https://doi.org/10.3141/1634-08.

Richards, P. I. 1956. "Shock waves on the highway." *Oper. Res.* 4 (1): 42–51. https://doi.org/10.1287/opre.4.1.42.

Seliman, S. M., A. W. Sadek, and Q. He. 2020. "Optimal variable, lane group-based speed limits at freeway lane drops: A multi-objective approach." *J. Transp. Eng. Part A: Syst.* 146 (8): 04020074. https://doi.org/10.1061/JTEPBS.0000395.

Smaragdis, E., M. Papageorgiou, and E. Kosmatopoulos. 2004. "A flow-maximizing adaptive local ramp metering strategy." *Transp. Res. Part B: Methodol.* 38 (3): 251–270. https://doi.org/10.1016/S0191-2615(03)00012-2.

Spiliopoulou, A., M. Kontorinaki, M. Papageorgiou, and P. Kopelias. 2014. "Macroscopic traffic flow model validation at congested freeway

off-ramp areas." *Transp. Res. Part C: Emerging Technol.* 41 (Apr): 18–29. https://doi.org/10.1016/j.trc.2014.01.009.

Srivastava, A., and N. Geroliminis. 2013. "Empirical observations of capacity drop in freeway merges with ramp control and integration in a first-order model." *Transp. Res. Part C: Emerging Technol.* 30 (May): 161–177. https://doi.org/10.1016/j.trc.2013.02.006.

Wang, Y., and M. Papageorgiou. 2006. "Local ramp metering in the case of distant downstream bottlenecks." In *Proc., IEEE Intelligent Transport System Conf.*, 426–431. New York: IEEE.

Wang, Y., X. Yu, S. Zhang, P. Zheng, J. Guo, L. Zhang, S. Hu, S. Cheng, and H. Wei. 2020. "Freeway traffic control in presence of capacity drop." *IEEE Trans. Intell. Transp. Syst.* 1–20. https://doi.org/10.1109/TITS.2020.2971663.

Yang, X., Y. Lu, and G. L. Chang. 2015. "Exploratory analysis of an optimal variable speed control system for a recurrently congested freeway bottleneck." *J. Adv. Transp.* 49 (2): 195–209. https://doi.org/10.1002/atr.1285.

Yuan, K., V. L. Knoop, and S. P. Hoogendoorn. 2015. "Capacity drop: Relationship between speed in congestion and the queue discharge rate." *Transp. Res. Rec.* 2491 (1): 72–80. https://doi.org/10.3141/2491-08.

Zhang, H. M., and S. G. Ritchie. 1997. "Freeway ramp metering using artificial neural networks." *Transp. Res. Part C: Emerging Technol.* 5 (5): 273–286. https://doi.org/10.1016/S0968-090X(97)00019-3.

Zhao, D., X. Bai, F. Y. Wang, J. Xu, and W. Yu. 2011. "DHP method for ramp metering of freeway traffic." *IEEE Trans. Intell. Transp. Syst.* 12 (4): 990–999. https://doi.org/10.1109/TITS.2011.2122257.